Using AI to Analyse Light Curves for GEO Object Characterisation

Emma Kerr, Elisabeth Geistere Petersen, Patrick Talon, David Petit
DEIMOS Space UK Ltd, Airspeed 1, 151 Eighth Street, Harwell Campus, OX11 0RL, UK
emma.kerr@deimos-space.com
Chris Dorn
Inverse Quanta Ltd, Brooklands, Pankridge Street, Crondall, Hampshire, GU10 5QU, UK
Stuart Eves
SJE Space Ltd., 29 Clayhill Road, Burghfield Common, Berkshire, RG7 3HB UK

ABSTRACT

Characterisation of space objects in Earth orbit is an essential task, particularly with the increase in space traffic and the advent of space traffic management. Proper understanding of an objects shape, size and attitude are vital in predicting its future behaviour. Light curves are increasingly being used to characterise objects, with methods ranging from simple regression analysis through to complex AI solutions. The method presented and demonstrated herein is a machine learning algorithm based on convolutional neural networks, capable of characterising object parameters such as geometry, attitude and materials of an object. The method is intended to be a flexible classification method, which could be extended to all orbits and any type of object, including debris. Herein, intermediate results of the ongoing study are presented, demonstrating the use of a multiclassification and multi-branch classification model. The results demonstrate that the method can successfully, with greater than 80% accuracy classify the shape, size, attitude and main material of an object in geosynchronous orbit from a single full night light curve.

1. INTRODUCTION

Characterisation of space objects is becoming increasingly important in an already congested and contested environment, set to become even more so. The primary reason for characterisation is for identification, and modelling purposes, understanding an objects geometry and attitude simplifies and removes assumptions from the modelling and prediction of that object's behaviour. However, other reasons can include political (such as treaty compliance), military (such as threat assessment) and research (such as developing better prediction models). Light curve data can be used to derive certain information about an object, but cannot yet answer all of these interests. Significantly, light curve data can be used to track patterns of life and detect changes in objects behaviour, particularly since light curve data is relatively easy and cheap to collect.

A light curve is made up of many data points of time stamped apparent magnitude. Analysis of the temporal variations in the light curve allow an analyst to derive characteristics of a spacecraft. With relatively basic regression techniques information on an objects rotation rate and likely attitude can be derived. With more involved analysis, such as proposed herein, much more can be derived, such as the geometry, and primary spacecraft materials. Due to the patterns seen in light curves of similar satellites, it was hypothesised that Artificial Intelligence (AI) could be used to analyse light curves and predict their characteristics, having been trained to recognise the correct patterns. Previous work [1], proved this hypothesis, while this paper discusses the improvements made since.

This paper discusses the latest results in an ongoing three-phase study. Phase 1 of the study consisted of a comprehensive literature review of potential methods for object characterisation, culminating in the selection of Machine Learning (ML) techniques. Phase 2 involved developing a light curve simulator to produce artificial light curves with which to train the AI and initial development of the ML algorithms. Phase 3, the current phase, involves an extensive observation campaign using optical sensors to gather real light curve data, and further development, testing and validation of the ML algorithms.

This study is focussed primarily on the characterisation of Geosynchronous Earth Orbit (GEO) objects, however, has been developed in such a way that the methodology could be applied to any region or spacecraft/debris with some minor modifications. The benefit of studying GEO objects, is they are always in view of the sensor, during operational hours, so long observations can be performed capturing full night light curves of objects at the same elevation angle.

Deimos owns and operates its own optical SST system, Deimos Sky Survey (DeSS). The observatory is sited in Puertollano, Spain. It currently consists of 4 operational and several prototype optical sensors, capable of tracking and surveillance of all orbital regions. Tracker 2 at DeSS, an optical sensor optimised for GEO object tracking, has been used to collect the light curves used in this project. The resolution of Tracker2 is 1.20 arcsec/pixel, when combined with the CCD. The CCD detector is used to captured very short exposure (< 1s) images, with a high frequency of 1 image every 2 seconds. Target objects are observed from dusk to dawn uninterrupted where possible, weather permitting etc. Some other systems, such as video cameras could obtain a higher sampling rate, however, they lack the sensitivity needed to capture images of GEO objects. The very short exposure time helps maintain high accuracy, avoiding conjunctions with background stars and maintaining rounded stars in the images (important for differential photometry). Target objects are not only tracked across full nights, but throughout the year too. The variation in solar aspect angle across the year produces variations in the light curves of the objects studied, allowing more information to be derived.

With the light curves collected by DeSS and those generated by the dedicated light curve simulator, it is possible to train the ML algorithm to predict object features using only the light curve. The success of the ML algorithm is primarily determined by the approach, herein neural networks (NN) are used. Both Convolutional Neural Networks (CNN) and Recurrent Neural Networks (RNN) are being studied, however, the results contained in this paper are from the work on CNNs only. The simulator is particularly important when considering a ML approach, since a large data set is needed to train the NN, and gathering the required volume of data would be expensive and time consuming. The simulator also has the important distinction of being able to simulate cases of objects which may be difficult to capture in real observations, such as various debris shapes. See [1] for more information on the development of the simulator.

2. OBSERVATION CAMPAIGN

Two observation campaigns were planned as part of this activity, a short campaign in Phase 2 and an extended one in Phase 3. The short campaign consisted of 16 nights of observations of a single satellite, Alphasat, used to validate the light curve simulator. The extended campaign involves a further 180 nights of observations (still ongoing), to be used in the development, testing and validation of the ML algorithms developed.

Alphasat was chosen for the short campaign as its operators, Inmarsat, were willing to share key information (or ground truth) on its geometry, position and attitude. This allowed the validation of the light curve simulator, as a simulated light curve could be compared to the real one gathered by DeSS, when they matched the simulator could be considered valid. Fig. 1 shows some of the light curves obtained in the short campaign, from Alphasat. Note the light curves have been shifted in magnitude (y-direction) to separate them and allow easy comparison.

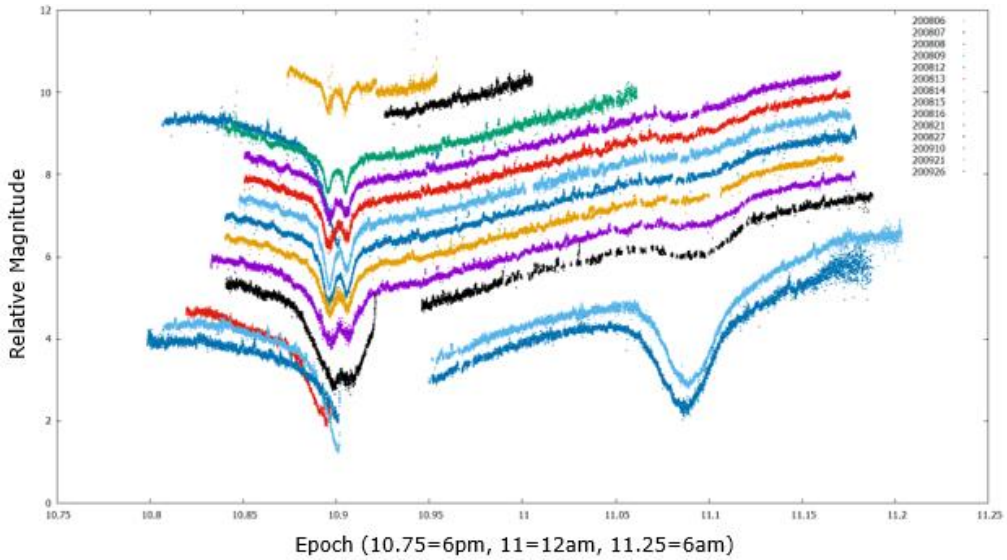

Fig. 1. Alphasat light curves gathered by Deimos Sky Survey. Note, light curves have been shifted in magnitude to allow comparison.

Of particular interest, is the differences in the light curves, having been taken over a period of 2 months, the variation in the solar aspect angle already alters the light curves. In previous work, it was posited that this would mean that a CNN would be incapable of identifying the characteristic of the object correctly, and an RNN would be needed. However, as will be seen in the results of this paper, this supposition was incorrect.

The long campaign is ongoing, with over 100 nights of observations completed at the time of this papers submission. Twenty-two target objects have been selected from the GEO ring, including Alphasat. Observations began in March 2021 and will end in November/December 2021. Some observation time was also dedicated to the observation of MEV-2 docking with Inmarsat 10-02 in January/February 2021. The campaign has been structured such that each of the 22 objects is observed for 1 full night each month.

3. DATA

The ML model development is based on real and simulated light curves. All of the samples are manually split into three subsets for training (70%), validation (15%) and testing (15%) of the model. The validation dataset is used during the model's training to assess its performances and adjust the hyperparameters where required. The testing dataset is used after the training to evaluate the final model's accuracy. The datasets are split before entry to the system, such that there can be no leakage of data between the three subsets.

The majority of the dataset consists of simulated data generated with various satellite configurations. These simulated light curves cover 5 different GEO orbits from the minimum to the maximum orbital distance. As in previous work [1], the data has been generated for four different cases: shapes, size, material and attitude, in which each subcase consists of one night of observation in each month. The real data used in the analysis herein consists of light curves from only the short campaign, from Alphasat. While this is currently a limited amount of real data, the number of samples will significantly increase with the observation campaign, which is ongoing.

Proportions of the labels available in the dataset can be seen in Fig. 2. For the shape and size cases, there is a reasonable balance between the different classes. However, for materials and attitude, there is a noticeable imbalance between the classes in both simulated and real data, as the base case for simulated data is configured with small size, aluminium material and north-south attitude. This imbalance is currently being addressed with new simulation cases.

Three main shape classifications are considered: box, sphere and box with wings (or solar panels). Four main materials are considered for the primary object body material, it is assumed the same material is always used for solar panels. Three main attitude modes are considered: 'ns', meaning the solar panels are aligned in to the north-south magnetic field lines; while 'ew' means the solar panels are aligned 90° rotated around the radius vector; and 'sun' where the object tracks the sun, not just the solar panels. Note in case where solar panels are present it is assumed they rotate on a single axis tracking the sun. Finally, four size classifications are considered: extra-small, small, medium and large.

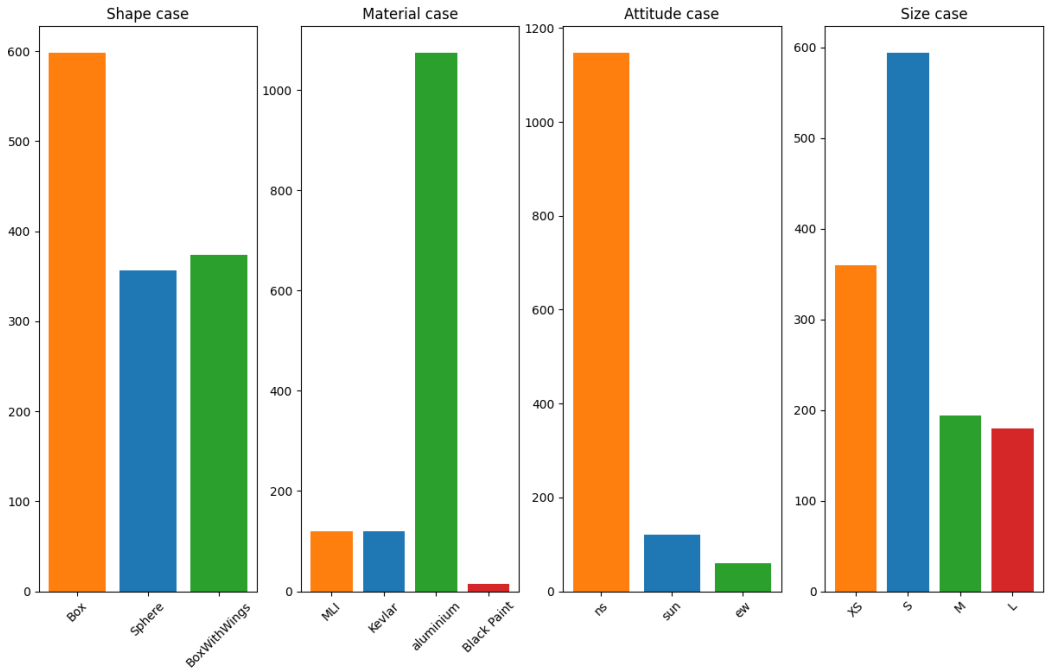

Fig. 2. Class balance in each case with both simulated and real light curves.

4. DATA PRE-PROCESSING

In order to prepare the data for ingestion into the ML algorithm, the real light curves are resampled to a constant frequency of two seconds, then both real and simulated cases are padded with zeros at the end of the sequence to ensure that all samples have a unified frequency and length. In order to scale the light curves to a range between 0 and 1, a predefined minimum and maximum values are set and used for all light curves in all the subsets. This gives a better representation of the magnitude range that the original light curves encompass, however has to be monitored for any new data not to have magnitude values higher or lower than the predefined value set. Note, this is a significant improvement made since the publication of previous results in [1], where data was normalised with no pre-set minimum and maximum, meaning that each light curves scaling was different, and the algorithm has difficulty distinguishing between sizes of objects.

5. AUTOENCODER

The autoencoder (AE) is an unsupervised learning model that is used for data compression and pattern extraction without the need of annotations for the input data. The autoencoder architecture includes an encoder and a decoder; the encoder reads the input data and extracts and stores meaningful features in an encoded format. The decoder takes this compressed sequence and attempts to reconstruct the data to its original form. The reconstructed signal that is produced by the decoder is used to test that the encoder is accurately encoding the signal. One of the use cases for the autoencoder is to pass the trained encoder into further machine learning algorithms, as will be discussed in the following section.

For this project, the AE consists of five convolutional layers each followed by max-pooling layers, and five up-sampling layers as seen in Fig. 3, and as detailed in [1]. The filter size for each layer is augmented by two in the encoder and decreased by two in the decoder to have an even parameter structure so the output would be in the same dimensions as the input. The kernel size was set to three for all convolutional layers. The activation function for all the CNN layers was set to be the ‘ReLu’ function, except for the output layer in the decoder, where a sigmoid function has been selected. The ‘Adam’ optimizer and Mean Square Error (MSE) loss function are used to train the model. A mask is added to the loss function in order to ignore missing data points and padding added to the input time series data. In addition, data augmentation methods are used during the AE model training to improve its robustness against short or long intervals of missing data points.

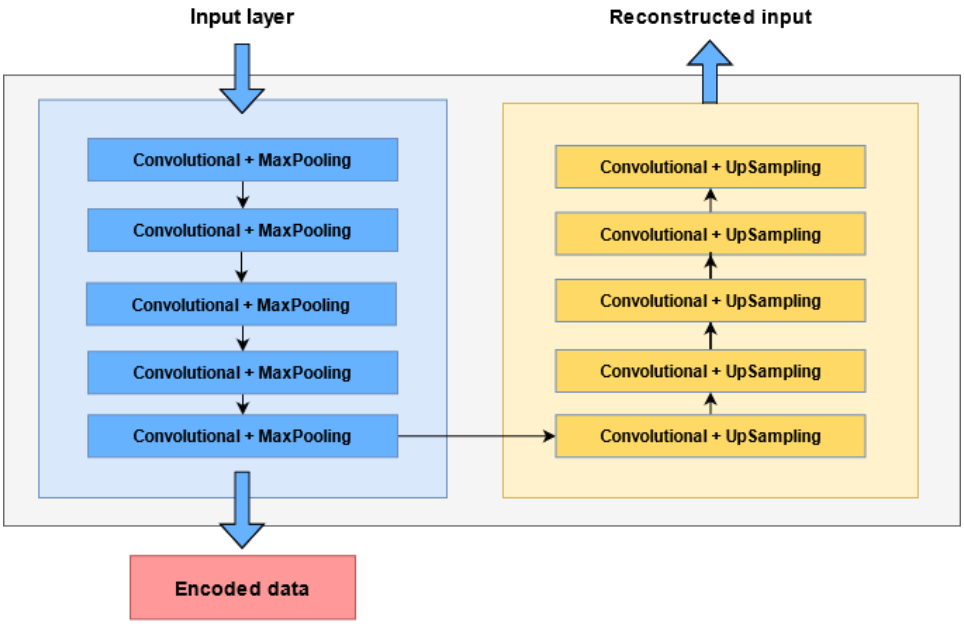

Fig. 3. A representation of the implemented autoencoder architecture.

6. CLASSIFICATION MODEL - CONVOLUTIONAL NEURAL NETWORK

A convolutional neural network is a deep learning algorithm that is built with convolutional layers. In the machine learning development process for this project [1], a model architecture from previous research work [2, 3] was implemented and adapted to learn and classify satellites shape, size, attitude and material from light curve data. The architecture contains 3 convolutional layers, all followed by a dropout and max-pooling layer. The parameters selected for these layers can be seen in Fig. 4, where values for filter and kernel size are defined in the convolutional layer, dropout rate in the dropout layer and pool size for the max-pooling layer. The pretrained encoder extracted from the autoencoder is added at the top of the algorithm to facilitate the feature extraction for the classifier. A notable improvement in model results can be seen for the multiclassification case of shape and size, which is discussed more in the following section.

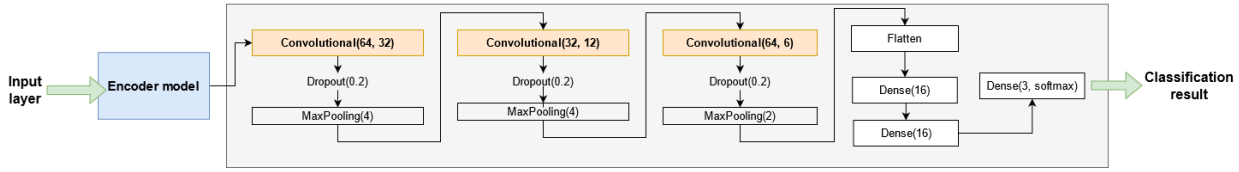

Fig. 4. Representation of the multiclassification model.

Further developments of the algorithm introduced a multi-branch model, which produces an independent output for each satellite's characteristic, as detailed in Fig. 5. This greatly improved time efficiency on the machine learning side as it can substitute the 4 individual models that only have an output for one class. The main architecture of this model stayed the same as described in the paragraph above, however it is important to note that for this model, the filter size in the convolutional layers was reduced by half, in order to increase the model's capability to be more generic and not overfit on the data sets. As seen in Fig. 5, the multi-branch model's last hidden dense layer is connected to 4 different output layers that independently classify an objects shape, size, material and attitude.

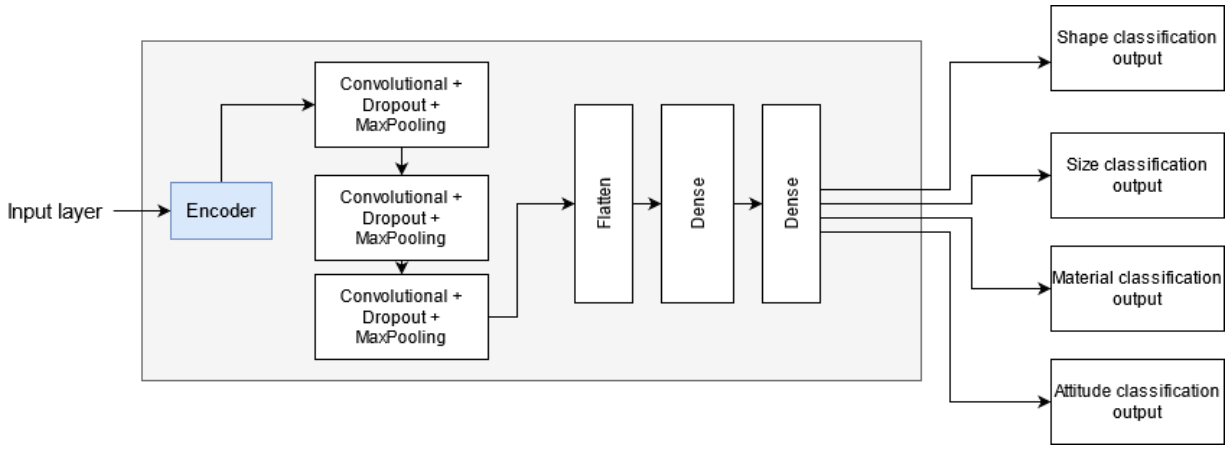

Fig. 5. A representation of the multi-branch model structure.

7. RESULTS

The results in Fig. 6 show the autoencoders precise reconstruction of the light curves for both the simulated and real data. In the real light curves as seen on the left in Fig. 6, the AE has captured a good reconstruction of the light curve pattern, as well as de-noising the time-series of any additional features like noise from the sequence. Missing and padded values are predicted with a constant random value, as the model is not trained to recognise these.

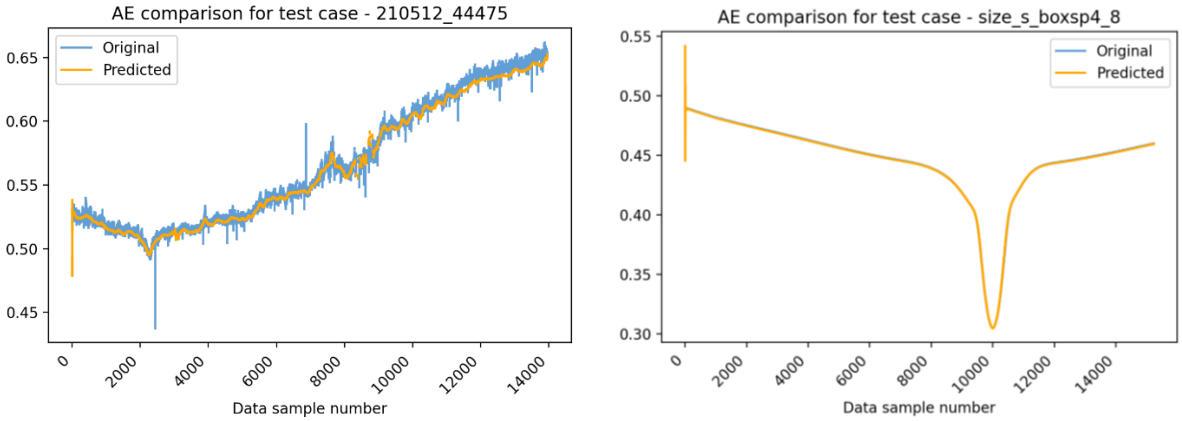

Fig. 6. Sample results of the autoencoder predictions on the test subset. Graph on the left shows the results of real light curve reconstruction and graph on right displays a sample of simulated data case. Note that the predicted constant value for the padding is masked in these plots for better visual representation of the results.

Previous work discussed the projects preliminary results [1], where the multiclassification model reached an overall accuracy of 33%. However, with the changes brought to the normalization of the data and with more training samples, the classification has now improved by 55% reaching an overall accuracy of 88%. Comparing the metrics between the 3 shapes, the model predicted with 100% accuracy for 'Sphere', 98.6% for 'Box' and 93.8% for 'BoxWithWings' satellites. For the size classes, the model has generally a good understanding. However, it can be seen in Fig. 7 that there are a few misclassifications, mainly for the extra-small ('XS') and medium ('M') cases 'Box' cases, where the shape is correctly classified but the size is not. The number of light curves included in training, validation and testing can be found in Table 1.

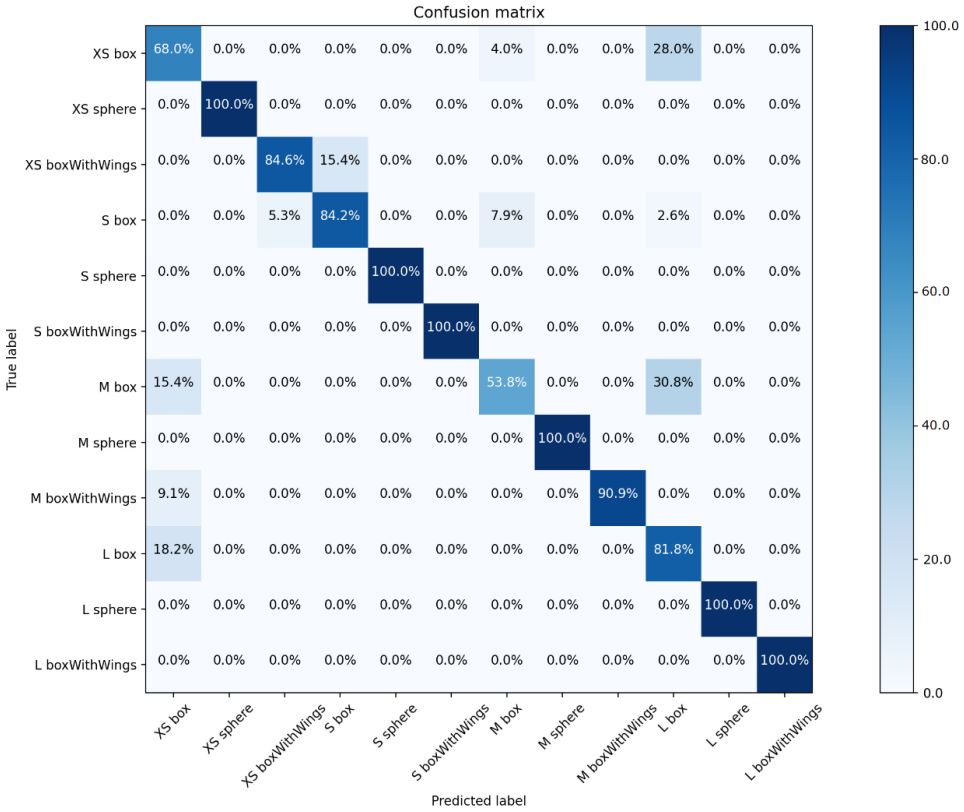

Fig. 7. Confusion matrix of the multiclassification model evaluated on the test subset.

Table 1. Dataset used in multiclassification model.

	Training			Validation			Testing			
Label	**Box**	**Sphere**	**Box with Wings**	**Box**	**Sphere**	**Box with Wings**	**Box**	**Sphere**	**Box with Wings**	**Total**
XS	43	184	39	7	31	8	10	25	13	360
S	120	161	136	31	39	22	25	38	22	594
M	41	39	52	6	8	11	13	13	11	194
L	44	36	41	5	13	7	11	11	12	180
Total										**1328**

For the multi-branch model, the results show promising performance for the classification of various target labels in each output branch. The shape case reaches an overall accuracy of 98.3% on the test subset with few cases being misclassified as either 'Box' or 'BoxWithWings', as seen in Fig. 8a. The Attitude and Size branches also display good results, as per Fig. 8b and Fig. 8c, attaining an accuracy of 94.8% and 84.2% respectively. For the material case, Fig. 8d most of the classes are predicted correctly, except for 'Black Paint'. This can be attributed to class imbalance as this label is the least represented in the training data. A possible solution, currently being tested with the on-going model developments, is to compute and implement class weights in the model training as this would help balance the bias to each class evenly. However, as previously mentioned more cases are also being added to address the case imbalance. The number of light curves included in training, validation and testing of each branch can be found in Table 2-Table 5.

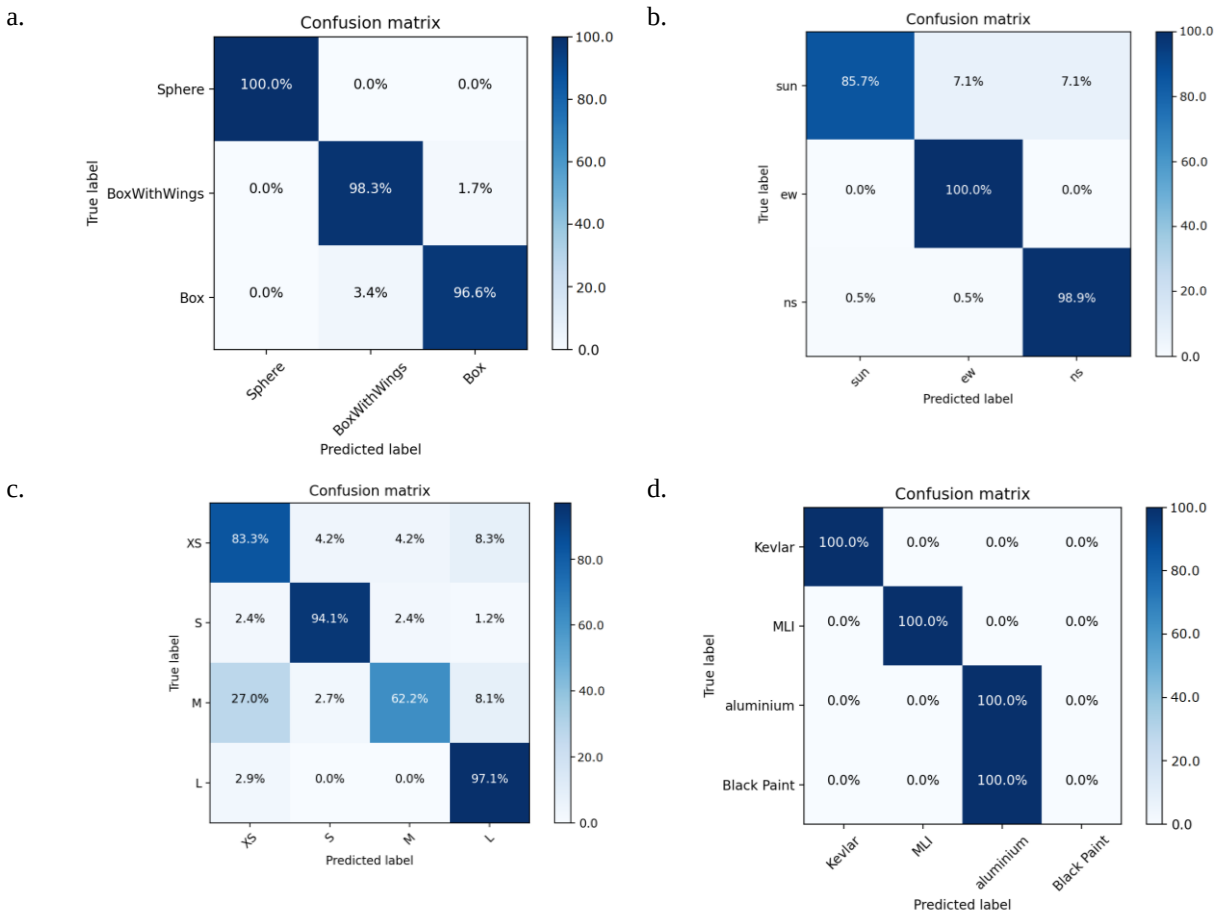

Fig. 8. Confusion matrices from multi-branch model evaluated on the test set. The model outputs consist of (a) shape branch, (b) attitude branch, (c) size branch and (d) material branch.

Table 2. Dataset used in multi-branch model, shape branch.

Label	Training	Validation	Testing	Total
Box	236	61	59	356
Sphere	423	88	87	598
Box With Wings	247	57	58	374
Total				**1328**

Table 3. Dataset used in multi-branch model, size branch.

Label	Training	Validation	Testing	Total
XS	266	46	48	360
S	422	87	85	594
M	118	39	37	194
L	112	34	34	180
Total				**1328**

Table 4. Dataset used in multi-branch model, attitude branch.

Label	Training	Validation	Testing	Total
Sun	92	15	14	121
EW	44	8	8	60

NS	782	183	182	1147
Total				**1328**

Table 5. Dataset used in multi-branch model, materials branch.

Label	Training	Validation	Testing	Total
Kelvar	82	19	19	120
MLI	82	19	19	120
Aluminium	742	167	165	1074
Black Paint	12	1	1	14
Total				**1328**

8. CONCLUSION AND FUTURE WORK

The results herein have demonstrated the successful use of an ML algorithm to classify an object, in terms of its shape, size, attitude and materials. While this study is not complete, these initial results are promising and prove that the method works. Major improvements have been made in the methodology since previous publication, and with further training and development, accuracy of classification could improve further.

Future work for this project includes training and testing the algorithm with more simulated cases, but also using the real data collected in the extended observation campaign. A regression model is also under development to predict an objects size, not just in label, but as an actual measurement.

9. ACKNOWLEDGEMENT

Deimos would like to thank the UK Defence Science & Technology Laboratory (Dstl) for funding this project.

10. REFERENCES

[1] E. Kerr, G. Falco, N. Maric, D. Petit, P. Talon, E. Petersen, C. Dorn, S. Eves, N. Sanchez-Ortiz, R. Dominguez Gonzalez, J. Nomen Torres. (2021) Light Curves for GEO Object Characterisation. 8th European Conference on Space Debris, 2021. Available at: https://conference.sdo.esoc.esa.int/proceedings/sdc8/paper/66

[2] R. Furfaro, R. Linares, V. Reddy. (2018). Space Objects Classification via Light-Curve Measurements: Deep Convolutional Neural Networks and Model-based Transfer Learning. Advanced Maui Optical and Space Surveillance Technologies Conference 2018. Available at: https://amostech.com/TechnicalPapers/2018/NROC/Furfaro.pdf

[3] R. Furfaro, R. Linares, V. Reddy. (2019) Shape Identification of Space Objects via Light Curve Inversion Using Deep Learning Models. Advanced Maui Optical and Space Surveillance Technologies Conference 2019. Available at: https://amostech.com/TechnicalPapers/2019/Machine-Learning-for-SSA-Applications/Furfaro.pdf